ICAS 2021 SHANGHAI
International Council of the Aeronautical Sciences
32nd Congress of the International Council of the Aeronautical Sciences
September 6-10, 2021 Pudong Shangri-La, Shanghai, China

AERODYNAMIC DESIGN OPTIMIZATION OF WAVERIDER-DERIVED VEHICLE

Su Wei[1], Dong Chao[1], Wang Xiaopeng[2], Zuo Yingtao[3]

[1] *Beijing Institute of Space Long March Vehicle, Beijing, 100076, China*
[2] *Shanghai Electro-Mechanical Engineering Institute, Shanghai, 201109, China*
[3] *National Key Laboratory of Aerodynamic Design and Research, Northwestern Polytechnical University, Xi'an, Shaanxi, 710072, China*

Abstract

Discrete adjoint method is adopted in an optimization of a waverider-derived vehicle. Free-form deformation parameterization method is used for the vehicle. Optimization results show that shock wave moves toward the vehicle after optimization, and lift-to-drag ratio increased by 21.3% compared to initial configuration. All these shows that the optimization is very successful.

Keywords: waverider, aerodynamic optimization, discrete adjoint

1. Introduction

Waverider is lifting body that is derived from a known analytical flowfield such as flow over a two-dimensional wedge or flow around a slender cone. The term 'Waverider' is used to describe a geometry that has an oblique shock attached to its leading edge nicely. By containing high pressure air under the vehicle, the waverider effectively rides on the wave, providing the potential for high lift-to-drag ratios relative to conventional designs.

Discrete adjoint method was widely used in acoustic, electromagnetics and transonic aerodynamic design problems, but it was rarely used in hypersonic vehicle optimization until recent years[1]. In this paper, a hypersonic vehicle model based on conic-flow waverider is developed. The aerodynamic performance is estimated with CFD method. The vehicle model is used to optimize maximum L/D with discrete adjoint method, in which control theory is applied directly to the set of discrete field equations. Since the time cost of discrete adjoint method is almost independent of design variables, it is quite suitable for design optimization with a lot of design variables. This paper gives maximum L/D optimization with restrictions of actual volumetric efficiency, which shows that this method is efficient for optimization of hypersonic vehicle.

The remainder of this paper is organized as follows: Section 2 describes flow solver and corresponding discrete adjoint method. Section 3 presents an improved grid deformation method based on the TFI and RBF methods. Section 4 gives the geometry parameterization of free form deformation. A lifting body is optimized by discrete adjoint method in section 5. The conclusions are drawn in section 6.

2. Flow analysis and sensitivity analysis method

The governing equations are the three-dimensional compressible Navier-Stokes equations. These equations describe the conservation of mass, momentum and total energy for a viscous compressible flow, which can be written as

$$\frac{d}{dt}\int_{\Omega} QdV + \int_{\partial\Omega} F \bullet \hat{n} dS = \int_{\partial\Omega} G \bullet \hat{n} dS \tag{1}$$

where Q is the set of conservative flow variables, F is the inviscid flux tensor, and G is the flux tensor associated with viscosity and heat conduction.

In this context, a multi-block viscous flow solver named LMNS3D[2] for steady and unsteady turbulent flows under the finite volume frame is employed. The equations are solved using a structured cell-centered finite-volume method. The discretization inviscid flux consists of central

scheme with scalar dissipation. Spalart-Allmaras one-equation turbulence model is used to compute the turbulent viscosity. These turbulent models are discretized and updated in a loosely-coupled way from the mean governing equation. For the time integration, LU-SGS implicit method is adopted.

Discrete adjoint[3] method is adopted to get the gradient of objective functions. The discrete residual of the nonlinear, multidimensional steady-state governing equations of the fluid and boundary conditions are approximated as a large system of coupled nonlinear algebraic equations as

$$R(Q(\mathrm{b}),\ X(\mathrm{b}),\ b) = 0 \tag{2}$$

where Q is the vector of converged steady field variables, X represents the computational grid, and b is the vector of independent input (design) variables. The aerodynamic characteristics of the vehicle are achieved by the integration of pressure over the surface grids. Similarly, the vector of aerodynamic output functions (objective functions) J depends on Q, X, and b. So J can be written symbolically as

$$J = J(Q(b),\ X(b),\ b) \tag{3}$$

Differentiate Eq. (2) and (3) with respect to b and we get

$$J' = \frac{\partial J}{\partial Q}Q' + \frac{\partial J}{\partial X}X' + \frac{\partial J}{\partial b} \tag{4}$$

$$R' = \frac{\partial R}{\partial Q}Q' + \frac{\partial R}{\partial X}X' + \frac{\partial R}{\partial b} = 0 \tag{5}$$

where $J' = \frac{dJ}{db}$, $R' = \frac{dR}{db}$, $Q' = \frac{dQ}{db}$, $X' = \frac{dX}{db}$, $\frac{dJ}{db} = [\frac{\partial J}{\partial b_1}, \frac{\partial J}{\partial b_2}, \cdots, \frac{\partial J}{\partial b_m}]$, and *m* is the number of design variables.

The governing equation Eq.(2) is added to objective function Eq.(3) as equality constraints and we get Lagrange equation

$$L(\mathrm{b}) = J(\mathrm{Q(b)}, X(\mathrm{b}), b) + \lambda^T \mathrm{R(Q(b)}, X(\mathrm{b}), \mathrm{b})$$

where λ is Lagrange multiplier and it can be any constant matrix. Differentiate L(b) with respect to b and then:

$$J' = L'(b) = \frac{\partial J}{\partial X}X' + \frac{\partial J}{\partial b} + \boldsymbol{\lambda}^T(\frac{\partial R}{\partial X}X' + \frac{\partial R}{\partial b}) + (\frac{\partial J}{\partial Q} + \boldsymbol{\lambda}^T\frac{\partial R}{\partial Q})\mathrm{Q}' \tag{6}$$

Since the choice of the Lagrange multiplier is arbitrary, the term Q' can be eliminated by solving the following Equation

$$\frac{\partial J}{\partial Q} + \lambda^T\frac{\partial R}{\partial Q} = 0 \tag{7}$$

Hence,

$$J' = \frac{\partial J}{\partial X}X' + \frac{\partial J}{\partial b} + \boldsymbol{\lambda}^{\mathrm{T}}(\frac{\partial R}{\partial X}X' + \frac{\partial R}{\partial b}) \tag{8}$$

As can be seen, all the gradient of objective functions J can be obtained once we get λ. The computational expense is independent on the number of design variables. Furthermore, it is proportional to the number of objective functions.

Eq.(7) is a linear algebraic equation which represents the discrete adjoint equation. A pseudo time term is added to Eq.(7) to enhance the diagonal dominance and the solution is obtained by marching in time, just like the flow solver.

$$(\frac{V}{\Delta t}I + \frac{\partial \tilde{R}}{\partial Q}^T)\Delta\lambda^n = -(\frac{\partial R}{\partial Q})^T\lambda^n + (\frac{\partial J}{\partial Q})^T$$

$$\Delta\lambda^n = \lambda^{n+1} - \lambda^n \tag{9}$$

where $\frac{\partial \tilde{R}}{\partial Q}$ is an approximation of the exact Jacobian matrix $\frac{\partial R}{\partial Q}$.

And then, Eq.(9) is resolved by GMRES method[4].

3. Moving Grid

The configuration of vehicle must be revised in every single iteration during the optimization, which means that we have to refresh the corresponding space grid to evaluate the aerodynamic characteristic during optimization. One of the direct methods is to generate new grid according to the new configuration automatically. But this method is very difficult to realize, especially for complex configurations. So it is very important to develop high efficient moving grid methodology. In the moving grid methodology, the new grids corresponding to the new configuration are efficiently generated according to two key points: one is the grid of initial configuration and the other is the changes between the new configuration and the initial configuration.

To preserve the original topo structure of the grid, Hounjet and Meijer's method is utilized[5]. Firstly, the displacements of vertices and edges in a multi-block grid are calculated according to displacements of the surface grid. Then transfinite interpolation (TFI) methodology is used to compute the displacements of the interior grid points in the block.

3.1 Radial Basis Functions Interpolation

The displacements of all the vertices and the edges in a multi-block grid can be calculated using the radial basis functions interpolation method as follows.

We know the displacements of vertices $\vec{x}_i$ on surface grid, which is assumed to be $\vec{d}_i$ (i=1,N, N is the number of vertices on surface grid). Then the displacement of any point $\vec{x}$ can be expressed as:

$$\vec{d}(\vec{x}) = \vec{a}_o + \sum_{i=1}^{N} \vec{a}_i R_i(\vec{x}_i)$$

where $R_i(\vec{x}_i) = \|\vec{x} - \vec{x}_i\|$. $R_i(\vec{x}_i)$ means the distance between space point $\vec{x}$ and vertices on surface grid of number i. The coefficient a_i (i=0,N)can be achieved according to $\vec{d}(\vec{x}_i) = \vec{d}_i$ and $\sum_{i=1}^{N} \vec{a}_i = 0$.

The displacements of all the vertices and the edges in a multi-block grid can be calculated using the above expressions.

3.2 Transfinite Interpolation

After we get the displacements of the vertices and the edges of the blocks, the displacements of the interior grid points of the multi-block grid is computed by transfinite interpolation. Then the grid of new configuration can be achieved by summing the displacements of all the grid points and the initial grid. More details can be found in [6].

4. Geometry Parameterization

The free form deformation (FFD) method is used to parameterize the vehicle in this paper. The FFD was proposed by Sederberg and Parry[7] in 1986 and then used in graphics processing, and now it is widely used by CAD and cartoon. Later it was introduced into vehicle design. FFD construct a $R^3 \to R^{'3}$ mapping function X=F(x) from physical space to parameter space, where x is logic coordinate of parameter space，X is coordinate of physical space. The deformation of vehicle in physical space is controlled by the movement of the control points of the parameter s, t, u by the following formula:

$$\boldsymbol{X}(s,t,u) + \Delta\boldsymbol{X}(s,t,u) = \sum_{i=1}^{l}\sum_{j=1}^{m}\sum_{k=1}^{n}\left[B_{l-1}^{i-1}(s)B_{m-1}^{j-1}(t)B_{n-1}^{k-1}(u)\right] \times \left[\boldsymbol{P}_{i,j,k} + \Delta\boldsymbol{P}_{i,j,k}\right] \tag{10}$$

where $\boldsymbol{P}_{i,j,k}$ and $\Delta\boldsymbol{P}_{i,j,k}$ are the matrixes representing the original coordinates and the displacements of the node point (i, j, k) of the control box, respectively. The number of control points of the hexahedral control box is l×m×n. (s,t,u) is the local curvilinear coordinates mapped into the control box, and it is also called lattice coordinates. $B_{l-1}^{i-1}(s)$ is the (i-1)-th Bernstein polynomial of degree l-1 defined as follows:

$$B_{l-1}^{i-1}(s) = \frac{(l-1)!}{(i-1)!(l-i)!} s^{i-1}(1-s)^{l-i} \tag{11}$$

In the matrix form, equation can be written as follows:

$$\Delta \boldsymbol{X} = B(s,t,u)\cdot \Delta \boldsymbol{P} \tag{12}$$

$$\begin{pmatrix} \delta x_1 \\ \delta x_2 \\ \delta x_3 \end{pmatrix} = \left(B_{1,1,1} \cdots B_{l.m.n} \right) \begin{bmatrix} \Delta P_{1,1,1,1} & \Delta P_{1,1,1,2} & \Delta P_{1,1,1,3} \\ \vdots & \vdots & \vdots \\ \Delta P_{l,m,n,1} & \Delta P_{l,m,n,2} & \Delta P_{l,m,n,3} \end{bmatrix} \tag{13}$$

where

$$B_{i,j,k} = B_{l-1}^{i-1}(s) B_{m-1}^{j-1}(t) B_{n-1}^{k-1}(u)$$

The procedures of FFD are listed as follows.

1) Construct control lattice around the objective to be parameterized.
2) Calculate the logic coordinate.
3) Move the control point of lattice.
4) Calculate the deformation of the vehicle with equation (10).

A parameterization software of vehicle is developed in our group. Typical interface is listed as follows. All of the definitions can be completed by interactive operation.

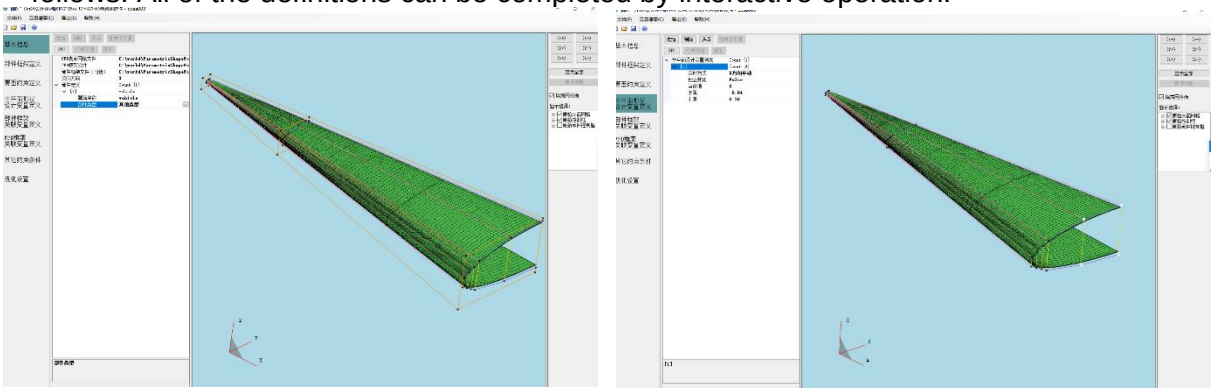

Figure 1 typical interface of the parameterization software

5. Optimization of waverider-derived vehicle

To demonstrate the approach developed in this paper, a hypersonic configuration similar to LEAC is considered. LEAC is a space plane configuration which has been developed in the Collaborative Research Center “Fundamental of Design of Aerospace Planes”(SFB 253) supported by the German Research Association (DFG) at Aachen University of Technology[8]. The length of this vehicle is 72m. the first 60% of the fuselage was intercepted and reduced 12 times. The final geometry is shown in Figure 2. The length of the fuselage is 3.6m, and the cross section of this fuselage is composed of two semi-ellipses. This configuration is called ELAC-X in the next.

The freestream Mach number is 6.0, and the flight altitude is 50Km. The Reynolds number is set to be 0.43×10^6. The grid size is 3.06 million. The reference area is set to be 1.737 m^2 for the semi-model. The cruise incidence is 8, and the corresponding lift coefficient is 0.108. Figure 1-Figure 3 displays surface grid and space grid of the vehicle.

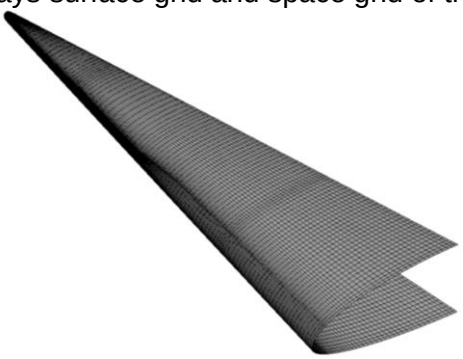

Figure 2 Surface grid of ELAC-X

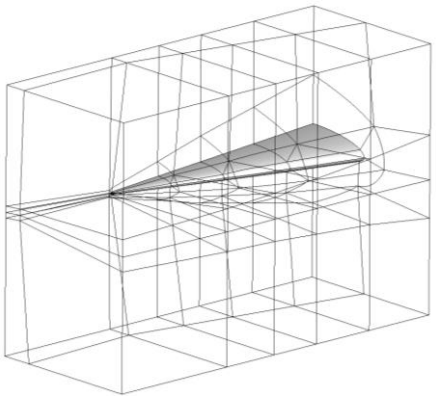

Figure 3 Space grid framework

Freeform deformation method is used to parameterize the vehicle. Figure 4 displays freeform

deformation framework (red lines). The plane of the vehicle can be optimized. One section as shown in Figure 4 (green section) was selected to be enlarged in span-wise direction. There are three sections in the FFD framework. The last two sections are selected to be optimized. Totally 13 design variables are selected including one plane design variable. The geometry constraint is that the volume of optimized vehicle is greater than 95% of the initial vehicle.

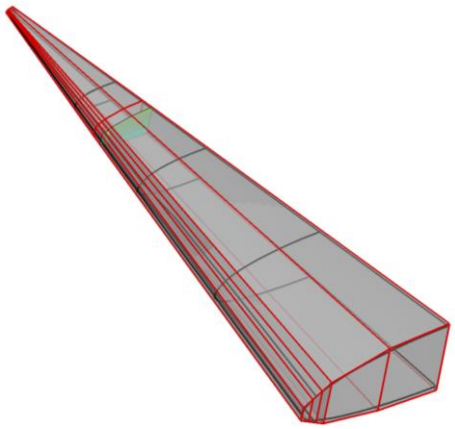

Figure 4 FFD framework of ELAC-X

The objective is to maximize L/D with fixed lift coefficient. Gradient-based optimization is completed. Totally 75 CFD evaluations is conducted during the optimization. The discretization inviscid flux consists of central scheme with scalar dissipation, but the optimized configuration is evaluated by a solver in which Roe scheme is adopted and is showed in this paper. Table 1 summarizes the design results at cruise condition. The lift-to-drag ratio is increased by 21.3% compared to the initial results. Figure 5-Figure 6 show the aerodynamic characteristic versus angle of attack and lift coefficient. Comparison of the framework and geometry before and after optimization is given in Figure 7 and Figure 8, in which the red line indicates the initial project. Figure 9-Figure 14 give the contour if the vehicle before and after optimization. As can be seen from all these results, the shock wave moves towards the vehicle after optimization. The optimization is successful.

Table 1 Optimization results

	C_l	Cd	K
Initial	0.1084	0.03162	3.43
Optimized	0.1084	0.02603	4.16

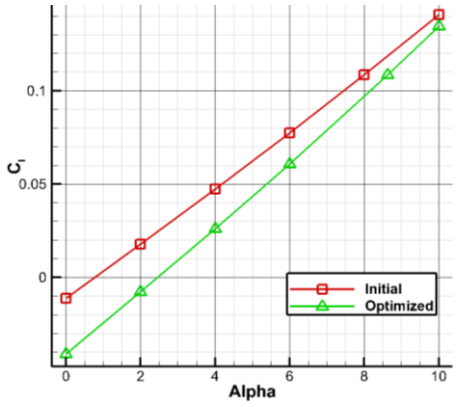

Figure 5 Lift coefficient comparison before and after optimization

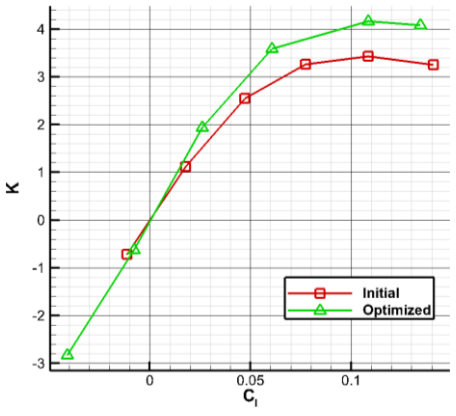

Figure 6 Lift-to-drag comparison before and after optimization

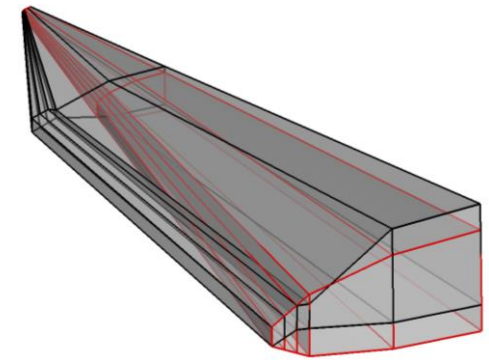

Figure 7 framework comparison before and after optimization

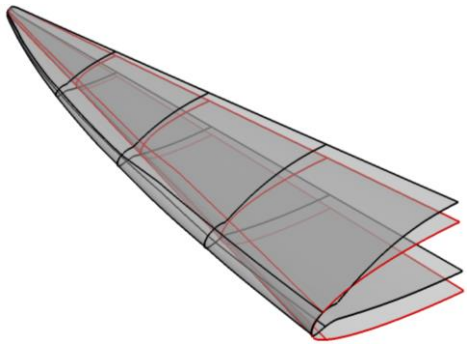

Figure 8 geometry comparison before and after optimization

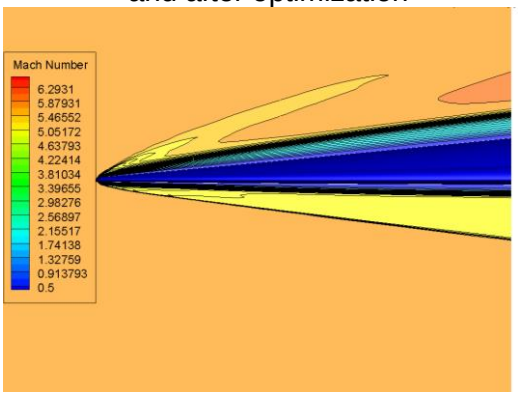

Figure 9 Mach contour of symmetry plane before optimization

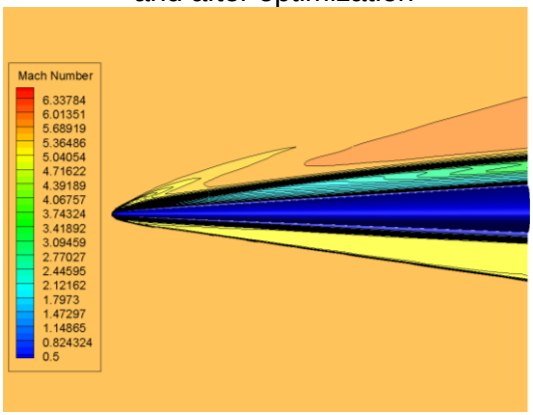

Figure 10 Mach contour of symmetry plane after optimization

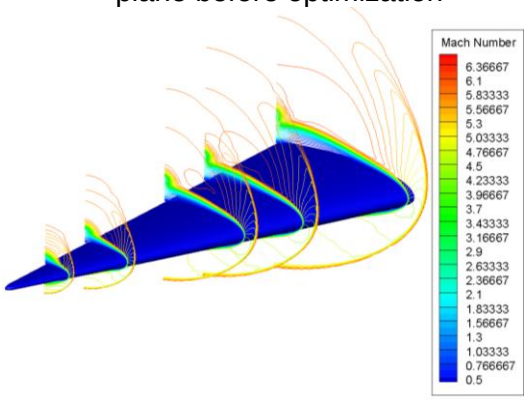

Figure 11 contour before optimization

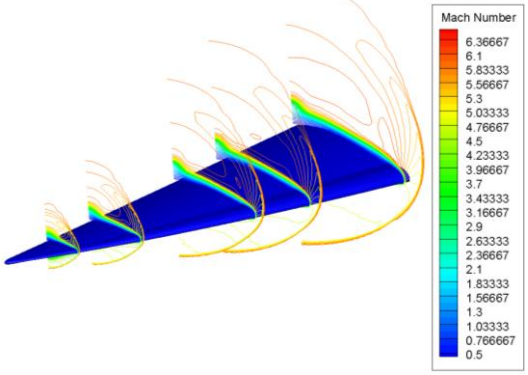

Figure 12 contour after optimization

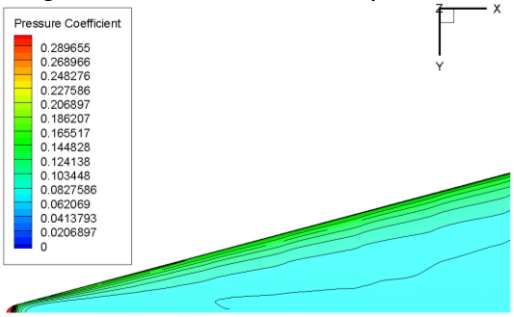

Figure 13 contour of lower surface before optimization

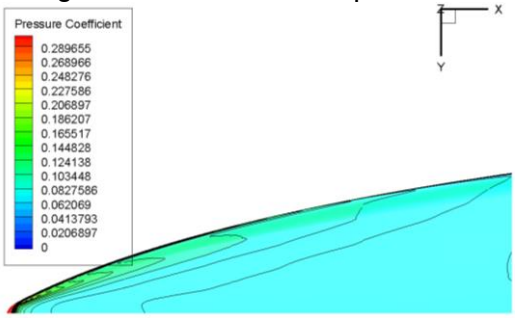

Figure 14 contour of lower surface after optimization

6. Conclusions

This paper tried to optimize a hypersonic vehicle with discrete adjoint method. Test show that this method can be used in hypersonic flow very well. Some detailed work will be done next, including

the stricter volume constraint.

Acknowledgments

This research was supported by a fund of the National Natural Science Foundation of China (General Program, 11772266).

7. Contact Author Email Address

Su wei: swsuwei@sina.com

8. Copyright Statement

References

[1] Kline H L and Alonso J J. Adjoint of Generalized Outflow-Based Functionals Applied to Hypersonic Inlet Design. AIAA Journal Vol. 55, No. 11,pp 3903-3915, 2017.

[2] Lin F, Zhonghong G, Kan X, Fang X, A Multi-block Viscous Flow Solver Based on GPU Parallel Methodology, Computers & Fluids, 95, pp. 19-39, 2014.

[3] Brian A L, and Dimitri J M. Parameter Sensitivity Analysis for Hypersonic Viscous Flow using a Discrete Adjoint Approach. AIAA 2010-447.

[4] Nemec M and Zingg D.W. Newton–Krylov Algorithm for Aerodynamic Design Using the Navier–Stokes Equations. AIAA Journal, Vol .40 ,No. 6,pp 1146-1154, 2002.

[5] Hounjet, M H L. and Meijer, J J. Evaluation of Elastomechanical and Aerodynamic Data Transfer Methods for Nonplanar Configurations in Computational Aeroelastic Analysis, Proceedings International Forum on Aeroelasticity and Structural Dynamics, Manchester, UK,1995.

[6] Yingtao Z, Gang C, Yueming L and Zhenghong G. Efficient Aeroelastic Design Optimization Based on the Discrete Adjoint Method. Transactions of The Japan Society for Aeronautical and Space Sciences,Vol.57, pp 343-351,2014.

[7] Sederberg T W., Parry S R. Freeform Deformation of Solid Geometric Models, Computer Graphics, vol.22, no. 4, pp.151-160, 1986.

[8] Krause E, Henze A. Recent progress in hypersonic: The ELAC Configuration, Pro. of the second European Symposium on Aerothermodynamics for Space Vehicles, 567-573, 1994.